2011 American Control Conference
on O'Farrell Street, San Francisco, CA, USA
June 29 - July 01, 2011

Vision-Based Cyclic Pursuit for Cooperative Target Tracking

Lili Ma and Naira Hovakimyan

***Abstract*— In this paper, we study the problem of cooperative target tracking among a group of ground robots. Cooperative target tracking control laws are presented that achieve tracking of a moving target with known position, velocity, and acceleration, for both single-integrator and double-integrator robot models. When the target's motion information are unknown constant, vision-based estimation schemes are applied to obtain estimates of the target's position and velocity. The effectiveness of the proposed control laws and their vision-based counterparts to achieve desired formations is demonstrated by numerical simulation examples using nonholonomic robots.**

Key Words: Cooperative target tracking, moving target, cyclic pursuit, vision-based estimation.

I. Introduction

Cooperative control of multiple autonomous agents has become an important topic of robotics and control theory research. The main theme is to analyze and synthesize spatially distributed control architectures to coordinate groups of autonomous agents. A typical assumption is that each agent communicates its position and/or velocity to its neighbors [1]–[10]. Among these, cyclic pursuit strategies, where each agent pursues its leading neighbor with the network topology forming a unidirectional ring, are particularly simple. Three pursuit formations can be achieved, i.e., rendezvous to a point, evenly-spaced circular formation, and evenly-spaced logarithmic spirals, depending on the value of a common offset angle and some control gains [2]. The results in [2] were extended in [4] from 2D to 3D and to the general network topology. Recent results in [9] allows the center of formation to be any point instead of being determined by the initial positions of the agents.

Cooperative target tracking is one form of motion coordination where a group of agents reach desired relative positions and orientations with respect to the target [11]. The problem considered in this paper is to achieve cooperative target tracking of a moving target with multiple mobile robots in pursuit formation. That is, the agents coordinate their motion to achieve the above-mentioned three collective formations to "capture" the target. Different from existing works that pursue a static point (or track a static target), we present coordinated control laws for a group of agents that track a target moving with known position, velocity, and acceleration. When the target's motion information are unknown, each agent is assumed to have monocular vision and estimates of the target's motion information will be used in the control laws to achieve the pursuit formations. Currently, we further assume that the target's velocity is an unknown constant when using vision-based estimates.

Similar to most of the work on coordinated control and cyclic pursuit [1]–[9], explicit communication among agents is required in this work. Computation of the control law is based on 1) communication among agents about the leading agent's position and velocity and 2) sensing and data processing carried out locally for estimation of the target's unknown size and unknown velocity by equipping each agent with a single camera. More specifically, a conventional pinhole camera is used and the camera is calibrated beforehand.

The paper is organized as follows. Section II reviews relevant cyclic pursuit strategies for both single and double integrators whose center of formation converges to any specified location. Section IV presents our cooperative target tracking control laws that achieve tracking of a moving target with known position, velocity, and acceleration, for both single-integrator and double-integrator robot models. When the target's motion information are unknown, estimation of the target's unknown velocity is presented in Sec. IV for two cases. The first case assumes that vision-based estimation is performed solely locally on each agent via a single camera. The second case assumes that the agent $i+1$ also sends its visual measurements to agent i such that a stereo-vision setup is formulated. Simulation results are shown in Sec. V. Finally, Section VI concludes the paper, discussing several remaining questions for future research.

II. Existing Results of Cyclic Pursuit

Consider n mobile robots in the plane, where agent i pursues the next $i+1$, modulo n. Let $\boldsymbol{x}_i(t) = [x_i(t),\, y_i(t)]^\top \in \mathbb{R}^2$ be the position of the agent i at time $t \geq 0$.

A. Single-Integrator Robot Model

If the kinematics of each agent is described by

$$\dot{\boldsymbol{x}}_i(t) = \boldsymbol{u}_i(t), \tag{1}$$

consider the following control input [9]

$$\boldsymbol{u}_i(t) = R(\vartheta)(\boldsymbol{x}_{i+1} - \boldsymbol{x}_i) - k_c \boldsymbol{x}_i, \quad k_c > 0, \tag{2}$$

Lili Ma is with Dept. of Electronics and Mechanical, Wentworth Institute of Technology, Boston, MA mal@wit.edu
Naira Hovakimyan is with Mechanical Science and Engineering, Univ. of Illinois at Urbana-Champaign, Urbana, IL nhovakim@illinois.edu

with the common offset angle $\vartheta \in [-\pi, \pi]$ and

$$R(\vartheta) = \begin{bmatrix} \cos\vartheta & \sin\vartheta \\ -\sin\vartheta & \cos\vartheta \end{bmatrix}. \quad (3)$$

The overall system can be written in compact form as [9]

$$\dot{\boldsymbol{x}}(t) = \underbrace{[L \otimes R(\vartheta) - k_c I_{2n}]}_{A(\vartheta)} \boldsymbol{x}(t), \quad (4)$$

where $\boldsymbol{x}(t) = [\boldsymbol{x}_1^\top(t), \boldsymbol{x}_2^\top(t), \ldots, \boldsymbol{x}_n^\top(t)]^\top$, L is the circular matrix

$$L = \begin{bmatrix} -1 & 1 & 0 & \ldots & 0 \\ 0 & -1 & 1 & \ldots & 0 \\ \vdots & & & \vdots & \\ 1 & 0 & 0 & \ldots & -1 \end{bmatrix}, \text{ and } I_{2n} = \begin{bmatrix} 1 & 0 \\ 0 & 1 \\ \vdots & \vdots \\ 1 & 0 \\ 0 & 1 \end{bmatrix}_{2n\times 2}. \quad (5)$$

It is shown in [9] that the control law in (2) constructs the cyclic pursuit strategy such that the agents' positions starting at any initial condition in $\mathbb{R}^2$ exponentially converge to formations centered at the origin. In particular, the agents' positions converge [9]:

1) if $0 \le |\vartheta| \le \pi/n$, to a single limit point;
2) if $\pi/n < |\vartheta| < 2\pi/n$:
   a) if $k_c > 2\sin(\pi/n)\sin(\vartheta - \pi/n)$, to a single limit point.
   b) if $k_c = 2\sin(\pi/n)\sin(\vartheta - \pi/n)$, to an evenly-spaced circle formation.
   c) if $k_c < 2\sin(\pi/n)\sin(\vartheta - \pi/n)$, to an evenly-spaced logarithmic spiral formation.

B. Double-Integrator Robot Model

If the dynamics of each agent are now described by a double-integrator model

$$\ddot{\boldsymbol{x}}_i(t) = \boldsymbol{u}_i(t), \quad (6)$$

the following feedback control law [9]

$$\begin{aligned} \boldsymbol{u}_i(t) = {} & KR(\vartheta)(\boldsymbol{x}_{i+1} - \boldsymbol{x}_i) + R(\vartheta)(\dot{\boldsymbol{x}}_{i+1} - \dot{\boldsymbol{x}}_i) \\ & - Kk_c\boldsymbol{x}_i - (K + k_c)\dot{\boldsymbol{x}}_i, \quad k_c > 0,\ K > 0, \end{aligned} \quad (7)$$

ensures that the agents' positions starting at any initial condition in $\mathbb{R}^2$ evolves exponentially to formations centered at the origin, if $-K$ is not an eigenvalue of $A(\vartheta)$ as defined in (4).

III. Tracking of a Moving Target

In this section, we present the cyclic pursuit control law to track a target that moves with known position, velocity, and acceleration where the agents are modeled by both single-integrator and double-integrator.

A. Single-Integrator Robot Model

Let $\boldsymbol{x}_t(t)$ denote the target's position and $\dot{\boldsymbol{x}}_t(t) = [v_x(t), v_y(t)]^\top$ be the target's velocity. We have the following results.

Theorem 1: For the single-integrator model in (1), the control law

$$\boldsymbol{u}_i(t) = R(\vartheta)(\boldsymbol{x}_{i+1} - \boldsymbol{x}_i) - k_c(\boldsymbol{x}_i - \boldsymbol{x}_t) + \dot{\boldsymbol{x}}_t,\ k_c > 0, \quad (8)$$

ensures that the agents' positions starting at any initial conditions exponentially converge to formations centered at the target's trajectory in the three pursuit formations described in Sec. II-A.

Proof. The proof is a simple consequence of Corollary 3.2.4 of [9]. The control law in (8) can be rewritten as

$$\boldsymbol{u}_i = R(\vartheta)[(\boldsymbol{x}_{i+1} - \boldsymbol{x}_t) - (\boldsymbol{x}_i - \boldsymbol{x}_t)] - k_c(\boldsymbol{x}_i - \boldsymbol{x}_t) + \dot{\boldsymbol{x}}_t. \quad (9)$$

Then the overall system consisting of the robot model (1) and the control law (8) can be rewritten in the compact form as

$$\dot{\boldsymbol{x}}(t) = A(\vartheta)(\boldsymbol{x}(t) - I_{2n}\,\boldsymbol{x}_t(t)) + I_{2n}\,\dot{\boldsymbol{x}}_t(t), \quad (10)$$

where $A(\vartheta)$ is given in (4). By letting

$$\boldsymbol{e}_i(t) = \boldsymbol{x}_i(t) - \boldsymbol{x}_t(t), \quad \boldsymbol{e}(t) = \boldsymbol{x}(t) - I_{2n}\,\boldsymbol{x}_t(t), \quad (11)$$

we have the error dynamics $\dot{\boldsymbol{e}}(t) = A(\vartheta)\,\boldsymbol{e}(t)$, which is in a similar form as (4). Thus, the agents' positions converge to pursuit formations centered at the target's positions $\boldsymbol{x}_t(t)$. This completes the proof. □

In summary, for the single-integrator robot model (1), the control law (8) guarantees cooperative tracking of a moving target via cyclic pursuit, that is via rendezvous to a point, evenly-spaced circle formation, or evenly-spaced logarithmic spirals, dependent on the values of ϑ and k_c. This control law requires that each agent knows its leader's motion information and the target's position and velocity.

B. Double-Integrator Robot Model

In the next, we extend the previous cyclic pursuit control law to double integrators. Consider the double-integrator model in (6) and let

$$\begin{aligned} \boldsymbol{v}_i(t) &= \dot{\boldsymbol{x}}_i(t), \\ \boldsymbol{v}_i^d(t) &= R(\vartheta)(\boldsymbol{x}_{i+1} - \boldsymbol{x}_i) - k_c(\boldsymbol{x}_i - \boldsymbol{x}_t) + \dot{\boldsymbol{x}}_t \end{aligned}$$

be the velocity and the desired velocity of agent i, respectively. Choosing $\boldsymbol{u}_i(t) = -K\boldsymbol{v}_i(t) + \boldsymbol{r}_i(t), \quad K > 0$ results in the first-order system

$$\dot{\boldsymbol{v}}_i(t) + K\boldsymbol{v}_i(t) = \boldsymbol{r}_i(t).$$

If we choose

$$\begin{aligned} \boldsymbol{r}_i(t) &= \dot{\boldsymbol{v}}_i^d(t) + K\boldsymbol{v}_i^d(t) \\ &= R(\vartheta)(\dot{\boldsymbol{x}}_{i+1} - \dot{\boldsymbol{x}}_i) - k_c(\dot{\boldsymbol{x}}_i - \dot{\boldsymbol{x}}_t) + \ddot{\boldsymbol{x}}_t \\ &\quad + KR(\vartheta)(\boldsymbol{x}_{i+1} - \boldsymbol{x}_i) - Kk_c(\boldsymbol{x}_i - \boldsymbol{x}_t) + K\dot{\boldsymbol{x}}_t, \end{aligned}$$

we have the following first-order differential equation:

$$\dot{\tilde{\boldsymbol{v}}}_i(t) + K\tilde{\boldsymbol{v}}_i(t) = \mathbf{0}, \tag{12}$$

where $\tilde{\boldsymbol{v}}_i(t) = \boldsymbol{v}_i(t) - \boldsymbol{v}_i^d(t)$. If $K > 0$, the error dynamics is exponentially stable. Therefore, the following control law applied to (6)

$$\begin{aligned} \boldsymbol{u}_i(t) &= -K\dot{\boldsymbol{x}}_i(t) + \boldsymbol{r}_i(t) \\ &= K[R(\vartheta)(\boldsymbol{x}_{i+1} - \boldsymbol{x}_i) - \dot{\boldsymbol{x}}_i] + R(\vartheta)(\dot{\boldsymbol{x}}_{i+1} - \dot{\boldsymbol{x}}_i) \\ &\quad - Kk_c(\boldsymbol{x}_i - \boldsymbol{x}_t) - k_c(\dot{\boldsymbol{x}}_i - \dot{\boldsymbol{x}}_t) + K\dot{\boldsymbol{x}}_t + \ddot{\boldsymbol{x}}_t, \end{aligned} \tag{13}$$

for $K > 0$ and $k_c > 0$ exponentially provides the vehicle velocity and guarantees globally stable rendezvous to a point, globally stable evenly-spaced circle formation, and globally stable evenly-spaced logarithmic spirals, depending on the values of ϑ, K, k_c, if $-K$ is not an eigenvalue of $A(\vartheta)$ as defined in (4).

IV. Vision-Based Estimation

The cyclic pursuit algorithm in (13) requires knowledge of the target's motion information. When the information are unknown, vision sensors can be used to obtain its estimates. In this section, vision-based estimation is formulated in a 2D setting (Fig. 1). It is further assumed that the target's velocity is constant and the target is within the sensing range of all agents. It is also assumed that some image processing algorithm is available to extract the subtended angle $\alpha_i(t)$ and the bearing angle $\beta_i(t)$ for the agent i. For the estimation task, the available information and measurements are:

1) The bearing angle $\beta_i(t)$ and the subtended angle $\alpha_i(t)$.
2) Each agent's own motion information from onboard sensors, i.e., its linear velocity and orientation.

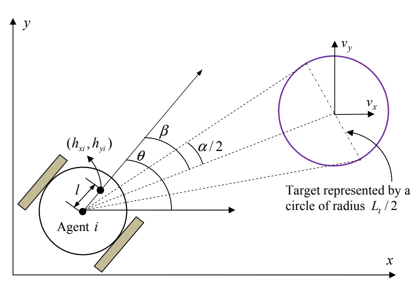

Fig. 1. Vision-based estimation.

Consider the motion of the vehicle and a target in the 2D Cartesian space. Let $\boldsymbol{z}_i(t) = [z_{ix}(t),\, z_{iy}(t)]^\top = \boldsymbol{x}_t(t) - \boldsymbol{x}_i(t)$ be the vector of relative position between the agent i and the target. In the kinematic setting, the relative dynamics can be described by:

$$\begin{bmatrix} \dot{z}_{ix}(t) \\ \dot{z}_{iy}(t) \end{bmatrix} = -v_i(t) \begin{bmatrix} \cos(\theta_i(t)) \\ \sin(\theta_i(t)) \end{bmatrix} + \begin{bmatrix} v_x \\ v_y \end{bmatrix}. \tag{14}$$

Recall that v_x, v_y are the components of the velocity vector of the target in the X and Y axis, respectively. Each agent has no knowledge of the target, including its velocity components v_x, v_y and its characteristic length L_t, except maybe for some conservative upper and lower bounds. Here, the subscript t denotes "target".

Assume that the bearing angle $\beta_i(t)$ and the subtended angle $\alpha_i(t)$ can be obtained by some image processing algorithm

$$\begin{cases} \beta_i(t) = \theta_i(t) - \arctan\left(z_{iy}(t)/z_{ix}(t)\right), \\ \alpha_i(t) = 2\arctan\left(L_t/(2d_i(t))\right), \end{cases} \tag{15}$$

where $d_i(t)$ is the relative range between the agent i and the target

$$d_i(t) = L_t/[2\tan(\alpha_i(t)/2)]. \tag{16}$$

With equations (15) and (16), the coordinates of the relative motion can be expressed as

$$\begin{bmatrix} z_{i,x}(t) \\ z_{i,y}(t) \end{bmatrix} = d_i(t) \begin{bmatrix} \cos(\theta_i(t) - \beta_i(t)) \\ \sin(\theta_i(t) - \beta_i(t)) \end{bmatrix}. \tag{17}$$

A. Estimation via Single Camera

It follows from equations (14) and (17) that

$$\begin{cases} \dfrac{\partial z_{ix}(t)}{\partial \alpha_i(t)}\dot{\alpha}_i(t) + \dfrac{\partial z_{ix}(t)}{\partial \beta_i(t)}\dot{\beta}_i(t) + \dfrac{\partial z_{ix}(t)}{\partial \theta_i(t)}\dot{\theta}_i(t) = v_x - \dot{x}_i(t), \\ \dfrac{\partial z_{iy}(t)}{\partial \alpha_i(t)}\dot{\alpha}_i(t) + \dfrac{\partial z_{iy}(t)}{\partial \beta_i(t)}\dot{\beta}_i(t) + \dfrac{\partial z_{iy}(t)}{\partial \theta_i(t)}\dot{\theta}_i(t) = v_y - \dot{y}_i(t). \end{cases} \tag{18}$$

Let the vector of unknown parameters be

$$\boldsymbol{\eta}_i(t) \triangleq [\eta_1(t),\, \eta_2(t),\, \eta_3(t)]^\top = [1,\, v_x,\, v_y]^\top / L, \tag{19}$$

where both the target's characteristic length L_t and its unknown velocity are assumed to be constant. Solving (18) for $\dot{\alpha}_i(t)$ and $\dot{\beta}_i(t)$ leads to

$$\begin{bmatrix} \dot{\alpha}_i(t) \\ \dot{\beta}_i(t) \end{bmatrix} = \underbrace{F(t) \begin{bmatrix} \dot{x}_i(t) & -1 & 0 \\ \dot{y}_i(t) & 0 & -1 \end{bmatrix}}_{w_i^\top(t)} \boldsymbol{\eta}_i(t) + \underbrace{\begin{bmatrix} 0 \\ \dot{\theta}_i(t) \end{bmatrix}}_{\boldsymbol{\varrho}_i(t)}, \tag{20}$$

where

$$F(t) = \begin{bmatrix} 4\sin^2(\frac{\alpha_i}{2})\cos(\theta_i - \beta_i) & 4\sin^2(\frac{\alpha_i}{2})\sin(\theta_i - \beta_i) \\ -2\tan(\frac{\alpha_i}{2})\sin(\theta_i - \beta_i) & 2\tan(\frac{\alpha_i}{2})\cos(\theta_i - \beta_i) \end{bmatrix}. \tag{21}$$

The estimation objective is to estimate the unknown parameter $\boldsymbol{\eta}_i(t)$ using visual measurements $\alpha_i(t), \beta_i(t)$ and the vehicle's own control $\dot{x}_i(t)$, $\dot{y}_i(t)$, and $\dot{\theta}_i(t)$.

It can be noticed that the matrix $w_i(t)$ and the vector $\boldsymbol{\varrho}_i(t)$ in (20) are known. As a result, the system in (20) exhibits the structure to which an existing nonlinear observer, the IBO in [12], can be applied to estimate $\boldsymbol{\eta}_i(t)$. To apply the IBO, the following assumption is needed.

Assumption 1: Let $\boldsymbol{m}_i(\tau)$ denote the i^{th} column of $w^\top(t)$ in (20). There are no nontrivial constants κ_i (for $i = 1, 2, 3$) such that $\sum_{i=1}^{3} \kappa_i \boldsymbol{m}_i(\tau) = 0$, for all $\tau \in [t,\, t+\mu]$, where $\mu > 0$ is a sufficiently small constant.

Let $\hat{\boldsymbol{\eta}}_i(t) = \hat{\boldsymbol{\eta}}_i(t) = [\hat{\eta}_1(t),\ \hat{\eta}_2(t),\ \hat{\eta}_3(t)]^\top$ be the estimate of $\boldsymbol{\eta}(t)$. The following observer can be designed for (20):

$$\begin{cases} \begin{bmatrix}\dot{\hat{\alpha}}_i(t)\\ \dot{\hat{\beta}}_i(t)\end{bmatrix} = GA_m \begin{bmatrix}\hat{\alpha}_i(t)-\alpha_i(t)\\ \hat{\beta}_i(t)-\beta_i(t)\end{bmatrix} + w_i^\top(t)\hat{\boldsymbol{\eta}}_i(t) + \boldsymbol{\varrho}_i(t), \\ \dot{\hat{\boldsymbol{\eta}}}_i(t) = -G^2 w_i^\top(t) P \left[\hat{\alpha}_i(t)-\alpha_i(t), \hat{\beta}_i(t)-\beta_i(t)\right]^\top, \end{cases} \tag{22}$$

where G is a scalar constant and A_m is a 2×2 Hurwitz matrix. The matrix P is the positive definite solution of the Lyapunov equation $A_m^\top P + PA_m = -Q$ for some choice of matrix $Q > 0$. According to Theorem 2.3 in [12] (page 65), there exists a positive constant G_0 such that choosing $G > G_0$ ensures the estimation errors $\hat{\boldsymbol{\eta}}_i(t) - \boldsymbol{\eta}_i(t)$ converge to zero exponentially.

B. Estimation via Stereo Vision

If agent $i+1$ communicates its visual measurements $\alpha_{i+1}(t)$, $\beta_{i+1}(t)$ to its partner agent i, the target's position can be computed based on these two agents' positions and visual measurements for agent i. In particular, the relative range between the target and agent i can be first computed, followed by the computation of the relative position $\boldsymbol{z}_i(t)$. This process is described next.

When agent i receives the visual measurements $\alpha_{i+1}(t)$ and $\beta_{i+1}(t)$ from agent $i+1$, we can have

$$\begin{aligned} \boldsymbol{x}_t &= \boldsymbol{x}_{i+1} + \frac{L_t}{2\tan(\alpha_{i+1}/2)}\left[\cos(\theta_{i+1}-\beta_{i+1}), \sin(\theta_{i+1}-\beta_{i+1})\right]^\top, \\ &= \boldsymbol{x}_i + \frac{L_t}{2\tan(\alpha_i/2)}\left[\cos(\theta_i-\beta_i), \sin(\theta_i-\beta_i)\right]^\top, \end{aligned} \tag{23}$$

which leads to

$$\boldsymbol{x}_i - \boldsymbol{x}_{i+1} = \frac{L_t}{2}\begin{bmatrix} \frac{\cos(\theta_{i+1}-\beta_{i+1})}{\tan(\alpha_{i+1}/2)} - \frac{\cos(\theta_i-\beta_i)}{\tan(\alpha_i/2)} \\ \frac{\sin(\theta_{i+1}-\beta_{i+1})}{\tan(\alpha_{i+1}/2)} - \frac{\sin(\theta_i-\beta_i)}{\tan(\alpha_i/2)} \end{bmatrix},$$

from where L_t can be computed by pseudo-inverse. Then the relative range $d_i(t)$ and the relative position $\boldsymbol{z}_i(t)$ can be computed from equations (16) and (17), respectively. Finally, the target's position can be obtained as $\boldsymbol{x}_t(t) = \boldsymbol{x}_i(t) + \boldsymbol{z}_i(t)$. As a result, the estimation problem reduces to estimating the target's unknown velocity, as detailed below, considering the relative dynamics in (14). These steps were described in [13] but are included here for the purpose of completeness.

Let

$$\bar{\boldsymbol{\eta}}_i(t) = [v_x,\ v_y]^\top, \quad \bar{\boldsymbol{\eta}}_i(0) = \bar{\boldsymbol{\eta}}_{i0}. \tag{24}$$

Since the moving ground target is a mechanical system, subject to Newton's second law, its velocity and acceleration are bounded. Thus there exist constants $\mu_{\bar{\eta}}$ and $d_{\bar{\eta}}$ such that

$$\begin{aligned} \|\bar{\boldsymbol{\eta}}_i(t)\| &\le \mu_{\bar{\eta}} < \infty, \quad \forall\ t \ge 0, \\ \|\dot{\bar{\boldsymbol{\eta}}}_i(t)\| &\le d_{\bar{\eta}} < \infty, \quad \forall\ t \ge 0. \end{aligned} \tag{25}$$

The estimates of the target's velocity (denoted by $\hat{v}_x(t)$ and $\hat{v}_y(t)$) can be obtained through the following steps [13], [14]:

1) State Predictor:

$$\begin{aligned} \dot{\hat{\boldsymbol{z}}}_i(t) &= A_m\tilde{\boldsymbol{z}}_i(t) - v_i(t)\left[\cos(\theta_i(t)), \sin(\theta_i(t))\right]^\top + \hat{\bar{\boldsymbol{\eta}}}_i(t), \\ \tilde{\boldsymbol{z}}_i(t) &= \hat{\boldsymbol{z}}_i(t) - \boldsymbol{z}_i(t), \quad \hat{\boldsymbol{z}}_i(0) = \boldsymbol{z}_{i0}, \end{aligned} \tag{26}$$

where A_m is a known Hurwitz matrix.

2) Update Law:

$$\dot{\hat{\bar{\boldsymbol{\eta}}}}_i(t) = \Gamma_c \operatorname{Proj}\left(\hat{\bar{\boldsymbol{\eta}}}_i(t), -P\tilde{\boldsymbol{z}}_i(t)\right),\ \hat{\bar{\boldsymbol{\eta}}}_i(0) = \hat{\bar{\boldsymbol{\eta}}}_{i0}, \tag{27}$$

where $\Gamma_c \in \mathbb{R}^+$ is the adaptation gain and P is the solution of the algebraic equation $A_m^\top P + PA_m = -Q$ for some choice of matrix $Q > 0$.

3) Low-Pass Filter: Let

$$\bar{\boldsymbol{\eta}}_{ie}(s) = [\bar{\eta}_{ie,1}(s),\ \bar{\eta}_{ie,2}(s)]^\top = C(s)\,\hat{\bar{\boldsymbol{\eta}}}_i(s),\ \bar{\boldsymbol{\eta}}_{ie}(0) = \hat{\bar{\boldsymbol{\eta}}}_{i0}, \tag{28}$$

where $C(s)$ is a diagonal matrix, whose i^{th} diagonal element $C_i(s)$ is a strictly proper, stable transfer function with low-pass gain $C_i(0) = 1$ for $i = 1, 2$, with s being the Laplace variable. Let $C_i(s) = \frac{c}{s+c}, \quad i = 1, 2, \quad c > 0$.

4) Extraction of $\hat{v}_x(t)$ and $\hat{v}_y(t)$ from $\bar{\boldsymbol{\eta}}_{ie}(t)$:

$$\hat{v}_x(t) = \bar{\eta}_{ie,1}(t), \quad \hat{v}_y(t) = \bar{\eta}_{ie,2}(t). \tag{29}$$

V. Simulation Results

Cyclic pursuit with vision-based estimation is implemented in Matlab using nonholonomic robots where each robot is described by the following state-space model:

$$\begin{bmatrix}\dot{x}_i(t)\\ \dot{y}_i(t)\\ \dot{\theta}_i(t)\\ \dot{v}_i(t)\\ \dot{\omega}_i(t)\end{bmatrix} = \begin{bmatrix} v_i(t)\cos(\theta_i(t))\\ v_i(t)\sin(\theta_i(t))\\ \omega_i(t)\\ 0\\ 0\end{bmatrix} + \begin{bmatrix} 0 & 0\\ 0 & 0\\ 0 & 0\\ 1/m & 0\\ 0 & 1/J\end{bmatrix}\begin{bmatrix}F_i(t)\\ \tau_i(t)\end{bmatrix}, \tag{30}$$

where $\boldsymbol{x}_i(t) = [x_i(t), y_i(t)]^\top$ is the inertial position of the robot i, $\theta_i(t)$ is the orientation, $v_i(t)$ is the linear velocity, $\omega_i(t)$ is the angular velocity, m is the mass, J is the moment of inertia, $F_i(t)$ is the force input, and $\tau_i(t)$ is the torque input. The objective is to maintain in formation the "hand" position of all agents, defined to be the point $\boldsymbol{h}_i(t) = [h_{ix}(t),\ h_{iy}(t)]^\top$ on distance $l \neq 0$ along the line that is normal to the wheel axis and intersects the wheel axis at the center point (Fig. 1). Applying the following feedback linearizing controller [2], [3]:

$$\begin{aligned} \begin{bmatrix}F_i(t)\\ \tau_i(t)\end{bmatrix} &= \begin{bmatrix}\frac{1}{m}\cos(\theta_i(t)) & -\frac{l}{J}\sin(\theta_i(t))\\ \frac{1}{m}\sin(\theta_i(t)) & \frac{l}{J}\cos(\theta_i(t))\end{bmatrix}^{-1} \\ &\left(\boldsymbol{u}_i(t) - \begin{bmatrix}-v_i(t)\omega_i(t)\sin(\theta_i(t)) - l\,\omega_i^2(t)\cos(\theta_i(t))\\ v_i(t)\omega_i(t)\cos(\theta_i(t)) - l\,\omega_i^2(t)\sin(\theta_i(t))\end{bmatrix}\right). \end{aligned} \tag{31}$$

the hand position dynamics becomes a double-integrator system given by $\ddot{\boldsymbol{h}}_i(t) = \boldsymbol{u}_i(t)$. Choosing $\boldsymbol{u}_i$ according to (13) achieve desired hand velocity for cooperative target tracking.

Choosing $\boldsymbol{u}_i(t)$ according to (13) provides the desired hand velocity for cooperative target tracking. Please see [3] for more details about this robot.

The following settings are used in the simulations:

1) Formation setup: $n = 6$, $\vartheta = 1.2\pi/n$.
2) Robot parameters: $m = 1$, $J = 1$, $l = 0.1$, $L_a = 1$, where L_a denotes the size of each robot.
3) Robot initial conditions:

$$\boldsymbol{x}_1(0) = [8.84,\ 14.90]^\top, \quad \boldsymbol{x}_2(0) = [-21.92,\ -0.93]^\top,$$
$$\boldsymbol{x}_3(0) = [-7.00,\ 11.90]^\top, \quad \boldsymbol{x}_4(0) = [-8.01,\ -6.96]^\top,$$
$$\boldsymbol{x}_5(0) = [-10.95,\ -0.04]^\top,\ \boldsymbol{x}_6(0) = [-1.94,\ -7.88]^\top.$$

4) Formation control parameters: $K = 1$ and

$$k_c = \begin{cases} 2\sin(\frac{\pi}{n})\sin(\vartheta - \frac{\pi}{n}) - 0.03, & \text{logarithmic}, \\ 2\sin(\frac{\pi}{n})\sin(\vartheta - \frac{\pi}{n}), & \text{circle}, \\ 2\sin(\frac{\pi}{n})\sin(\vartheta - \frac{\pi}{n}) + 0.08, & \text{point}. \end{cases} \tag{32}$$

5) Target parameters:

$$[v_x, v_y]^\top = [0.5,\ 0.5]^\top,\ \boldsymbol{x}_t(0) = [-6,\ 2]^\top,\ L_t = 2.$$

6) IBO parameters: $A_m = -\mathbb{I}_2,\ P = \mathbb{I}_2/2,\ G = 10.$
7) Fast estimator:$A_m = -\mathbb{I}_2, P = \mathbb{I}_2/2, \Gamma_c = 10^6, c = 2.$

Simulation is first performed using the control laws described in Sec. III-B. Figure 2 shows convergence from random initial positions to the target trajectory via an evenly-spaced circular formation, an evenly-spaced logarithmic spiral, and rendezvous to a point, using the formation control parameters in (32). In each scenario, trajectories of the 6 agents are plotted together with the trajectory of the target and the center trajectory of all agents.

Since the circular formation is more appropriate for cooperative target tracking, attention is given to this type of formation hereafter. Fig. 3(a) shows the average formation radius of case (a) in Fig. 2, where the radius converges to a constant. In Fig.3(b), the relative angle between agent i and agent $i+1$ for $i = 1, 2, \ldots, n$ are plotted in degree. Since all these angles converge to $60°$ which equals $360/n$, the six agents span evenly on a circle. In summary, Fig. 3 shows successful achievement of the circular formation while tracking the moving target. Later simulations are focused on the circular formation as well.

Figure 4 shows the simulation results of cooperative target tracking when the target's motion information are estimated using the method in Sec. IV-A. The trajectories of all agents in Fig.4(a) shows that the team tracks the target while maintaining a circular motion around the target. It is also shown in Fig. 4(b) and (c) that the estimated target velocity components converge to their true values for all the 6 agents.

Figure 5 shows the cooperative target tracking using the stereo-vision type estimation method described in Sec. IV-B, where agent $i+1$ sends its visual measurements to agent i.

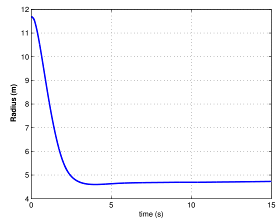

(a) Average Formation Radius

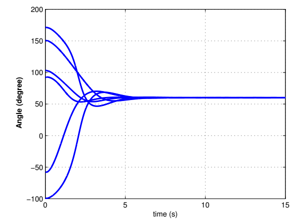

(b) Relative Angle Between Agents i and $i+1$

Fig. 3. Average formation radius and relative angles between agents for the circular formation using known target motion information.

It can be seen from Fig. 5(a) that the circular formation and target tracking are also achieved. However, simulation results shown in (b) and (c) show that the estimation seems to be more sensitive to noise. Notice that the estimation method in Sec. IV-B is able to estimate time-varying target velocity, though the simulation results shown in Fig. 5 assume that the target moves with constant velocity, that is, $\ddot{\boldsymbol{x}}_t(t) = 0$.

VI. Conclusion

This paper considers cooperative target tracking that is inspired by the idea of cyclic pursuit. Cooperative target tracking control laws are presented for both single-integrator and double-integrator robot models when the target's motion information are known. If the target's motion information are unknown, vision-based estimation schemes are applied, assuming that each robot has monocular vision. The effectiveness of the proposed vision-based control laws to achieve the desired formations is demonstrated by numerical simulation examples using a nonholonomic robot model described in the literature.

This work leaves several questions for future investigations. First, the formation control laws and estimation schemes can be extended to 3D case. Second, it looks to us that the stereo-type estimation scheme that uses computed target positions seems to be sensitive to measurement noise. We think that formulation of the estimation task in terms of the original visual measurements can help to resolve this issue. Third, the proposed formation control laws cannot specify the radius of formation. Being able to specify the formation radius would be a desirable feature in the context of target tracking. Finally, the collision avoidance capability needs to be added to the team robots for real applications.

References

[1] A. Jadbabaie, J. Lie, and A. Morse, "Coordination of groups of mobile autonomous agents using nearest neighbor rules," *IEEE Transactions on Automatic Control*, vol. 48, no. 6, pp. 988–1001, June 2003.

[2] M. Pavone and E. Frazzoli, "Decentralized policies for geometric pattern formation and path coverage," *ASME Journal of Dynamic Systems, Measurement, and Control*, vol. 129, no. 5, pp. 633–643, 2007.

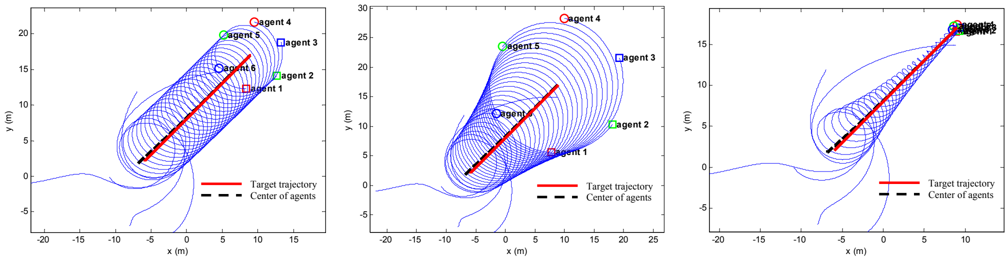

(a) Circular Formation (b) Logarithmic Spiral (c) Rendezvous to a Point

Fig. 2. Cooperative tracking of a moving target with known position and velocity via cyclic pursuit.

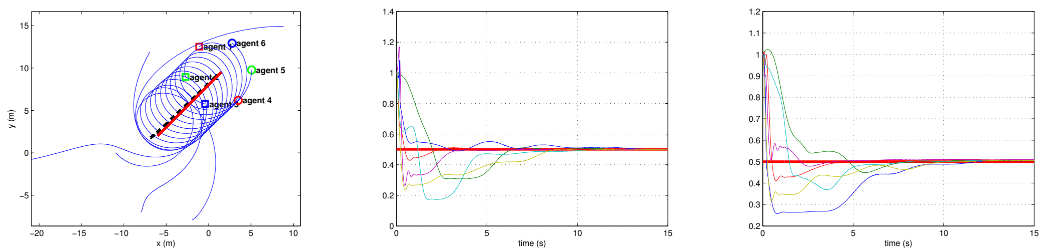

(a) Circular Formation (b) Estimation of v_x (c) Estimation of v_y

Fig. 4. Cooperative tracking of a moving target with estimated target motion information using the scheme in Sec. IV-A.

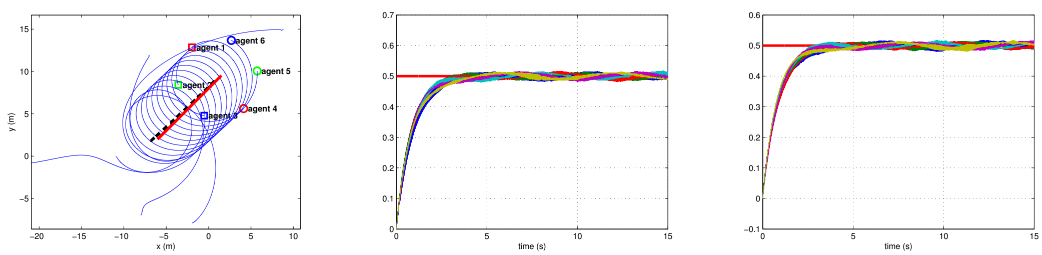

(a) Circular Formation (b) Estimation of v_x (c) Estimation of v_y

Fig. 5. Cooperative tracking of a moving target with estimated target motion information using the scheme in Sec. IV-B.

[3] J. Lawton, R. Beard, and B. Young, “A decentralized approach to formation maneuvers,” *IEEE Transactions on Robotics and Automation*, vol. 19, no. 6, pp. 933–941, Dec. 2003.

[4] W. Ren, “Collective motion from consensus with cartesian coordinate coupling,” *IEEE Transactions on Automatic Control*, vol. 54, no. 6, pp. 1330–1335, June 2009.

[5] J. Marshall, M. Broucke, and B.Francis, “Pursuit formations of unicycles,” *Automatica*, vol. 42, pp. 3–12, 2006.

[6] A. Sinha and D. Ghose, “Generalization of linear cyclic pursuit with application to rendezvous of multiple autonomous agents,” *IEEE Transactions on Automatic Control*, vol. 51, no. 11, pp. 1819–1824, Nov. 2006.

[7] J. Marshall, M. Broucke, and B. Francis, “Formations of vehicles in cyclic pursuit,” *IEEE Transactions on Automatic Control*, vol. 49, no. 11, pp. 1963–1974, Nov. 2004.

[8] W. Dong and J. Farrell, “Cooperative control of multiple nonholonomic mobile agents,” *IEEE Transactions on Automatic Control*, vol. 53, no. 6, pp. 1434–1448, July 2008.

[9] J. Ramirez, “New decentralized algorithms for spacecraft formation control based on a cyclic approach,” Ph.D. dissertation, Massachusetts Institute of Technology, Boston, 2010.

[10] N. Moshtagh, N. Michael, A. Jadbabaie, and K. Daniilidis, “Vision-based, distributed control laws for motion coordination of nonholonomic robots,” *IEEE Transactions on Robotics*, vol. 25, no. 4, pp. 851–860, 2009.

[11] Y. Lan, G. Yan, and Z. Lin, “A hybrid control approach to cooperative target tracking with multiple mobile robots,” in *American Control Conference*, MO, June 2009, pp. 2624–2629.

[12] M. Jankovic and B. Ghosh, “Visually guided ranging from observations of points, lines and curves via an identifier based nonlinear observer,” *Systems and Control Letters*, vol. 25, pp. 63–73, 1995.

[13] L. Ma and N. Hovakimyan, “Cyclic pursuit with vision-assisted estimation,” in *American Control Conference*, Baltimore, July 2010, pp. 5532–5537.

[14] L. Ma, C. Cao, N. Hovakimyan, C. Woolsey, and W. Dixon, “Fast estimation for range identification in the presence of unknown motion parameters,” *IMA Journal of Applied Mathematics*, vol. 75, pp. 165–189, Feb. 2010.